

Spin-Flip Raman Scattering by Carriers in PbTe, PbSe, and PbS

SUDHANSHU S. JHA*

IBM Watson Research Center, Yorktown Heights, New York, 10598

(Received 21 November 1968)

Because of spin-orbit coupling, an incident light wave can flip the effective spin of carriers in a semiconductor. In the presence of a strong dc magnetic field H , the frequency shift for the scattered light due to this process corresponds to the intraband excitation energy $g_{\text{eff}}\beta H$. Using the band-edge structure of PbTe, PbSe, and PbS at the L point in the Brillouin zone, the spin-flip Raman cross sections are calculated for both electrons and holes in these materials. Scattering amplitudes, which can be assumed to be independent of the magnetic field, are calculated by considering six bands near the band gap. The predictions of a simple two-band model including the spin-orbit effect are also analyzed to try to relate the scattering amplitudes directly to energy gaps and effective masses. Theoretical values for the cross sections in PbTe and PbSe for a CO_2 laser are comparable to those in InSb. The nature of the variation of these cross sections with the carrier concentration n and the magnetic field H is discussed.

I. INTRODUCTION

IN presence of a strong dc magnetic field, inelastic scattering of light from intraband excitations of electrons¹ in InSb and InAs has been observed experimentally² with a CO_2 laser. Using Kane's band structure for InSb and InP near the Γ point, Yafet³ has derived expressions for cross sections for the Landau-Raman (LR) process, where the spin-direction remains the same ($\Delta S=0$) but Landau-level quantum number changes ($\Delta l=1$, $\Delta l=2$), and for the spin-flip Raman (SFR) process where only the spin quantum number changes ($\Delta S=1$, with corresponding excitation energy $g_{\text{eff}}\beta H$). Recently, Patel and Slusher⁴ have reported the observation of SFR scattering in PbTe. Mixed processes have not yet been observed consistently.

In the electric-dipole approximation there is no LR scattering from electrons in a simple parabolic band, because in this case Landau levels are equally spaced, with electronic motion harmonic. Also, in absence of spin-orbit coupling SFR scattering vanishes since the dominant $\mathbf{A}\cdot\mathbf{P}$ interaction of the light wave cannot flip the electronic spin. Thus for appreciable LR scattering it is essential to use semiconductors with highly non-parabolic bands whereas for large SFR scattering, one has to choose materials with large spin-orbit coupling. For LR scattering, it is also clear that numerical results for the cross section will be very sensitive to the detailed variation of the energy of an electron near the band-edge and its necessarily complicated motion in the dc magnetic field. However, for low magnetic fields SFR scattering amplitude is independent of the dc field³ and it is enough to know the band-edge structure in the effective-mass approximation. In this paper we will

calculate SFR cross sections for lead salts using band-structure parameters obtained by Lin and Kleinman.⁵

In Sec. 2 we will review the band structure of PbTe, PbSe, and PbS at the L point in the presence of the spin-orbit coupling and discuss the structure of momentum matrix elements between six levels (each Kramers doublet in absence of the magnetic field) near the band gap. Since in the first approximation the effect of the dc field on the matrix elements can be neglected in our case, we use these to calculate the spin-flip transition amplitudes and scattering cross sections for both electrons and holes in these materials in Sec. 3. Numerical results are obtained by using the values for band-structure parameters due to Lin and Kleinman⁵ based on the pseudopotential method. Since these parameters for PbTe differ from the corresponding values obtained by Conklin, Johnson, and Pratt⁶ based on a true potential, we also consider a simple two-level approximation in Sec. 4 and obtain the cross sections directly from the experimental values of the bandgaps and effective masses. The calculated cross sections are large in both PbTe and PbSe and are of the same order as in InSb. We will discuss our results in Sec. 5.

II. BAND-EDGE STRUCTURE

Each of the lead salts under consideration has the NaCl crystal structure (fcc) with a truncated octahedron as the Brillouin zone. From available experimental as well as theoretical results it has been established that conduction- and valence-band extrema are located at the L point (111 edge) of the Brillouin zone. The lowest set of states, (L_1, L_2') , for an empty fcc lattice,^{7,8} at the L point arises from linear combinations of two plane-wave states of wave vectors $\mathbf{k}=\pm(2\pi/a)(\frac{1}{2}, \frac{1}{2}, \frac{1}{2})$. The next set of six states $[L_1, L_2', L_3(2), L_3'(2)]$ arising from linear combinations of plane waves of wave vectors

* On leave from Tata Institute of Fundamental Research, Bombay, India.

¹ P. A. Wolff, Phys. Rev. Letters **16**, 225 (1966).

² R. E. Slusher, C. K. N. Patel, and P. A. Fleury, Phys. Rev. Letters **18**, 530 (1967); C. K. N. Patel and R. E. Slusher, Phys. Rev. **167**, 413 (1968).

³ Y. Yafet, Phys. Rev. **152**, 858 (1966).

⁴ C. K. N. Patel and R. E. Slusher, Bull. Am. Phys. Soc. **13**, 480 (1968).

⁵ P. J. Lin and L. Kleinman, Phys. Rev. **142**, 478 (1966).

⁶ J. B. Conklin, L. E. Johnson, and G. W. Pratt, Phys. Rev. **137**, A1282 (1965). See other references in this paper.

⁷ See, e.g., C. Kittel, *Quantum Theory of Solids* (John Wiley & Sons, Inc., New York, 1963), p. 213.

⁸ J. O. Dimmock and G. B. Wright, Phys. Rev. **135**, A821 (1964).

$\mathbf{k} = \pm(2\pi/a)(\frac{1}{2}, \frac{1}{2}, \frac{3}{2})$, $\pm(2\pi/a)(\frac{3}{2}, \frac{1}{2}, \frac{1}{2})$ and $\pm(2\pi/a)(\frac{1}{2}, \frac{3}{2}, \frac{1}{2})$ determines the structure of the bands near the gap. If we include the spin, we may label the basis functions by $L_{6\uparrow}^+(L_1)$, $L_{6\downarrow}^+(L_1)$; $L_{6\uparrow}^+(L_3)$, $L_{6\downarrow}^+(L_3)$; $L_5^+(L_3)$, $L_4^+(L_3)$; $L_{6\uparrow}^-(L_2')$, $L_{6\downarrow}^-(L_2')$; $L_{6\uparrow}^-(L_3')$, $L_{6\downarrow}^-(L_3')$; $L_5^-(L_3')$, $L_4^-(L_3')$. In terms of the plane waves

$$\phi_1 = \exp[(i\pi/a)(-x-y+3z)],$$

$$\phi_2 = \exp[(i\pi/a)(3x-y-z)],$$

$$\phi_3 = \exp[(i\pi/a)(-x+3y-z)],$$

we may write

$$L_{6\uparrow}^+(L_1) = (1/\sqrt{6})[(\phi_1 + \phi_1^*) + (\phi_2 + \phi_2^*) + (\phi_3 + \phi_3^*)]\uparrow,$$

$$L_{6\downarrow}^+(L_1) = K L_{6\uparrow}^+(L_1),$$

$$L_{6\uparrow}^+(L_3) = (1/\sqrt{6})$$

$$\times [(\phi_1 + \phi_1^*) + (\phi_2 + \phi_2^*)\omega^* + (\phi_3 + \phi_3^*)\omega]\uparrow,$$

$$L_{6\downarrow}^+(L_3) = K L_{6\uparrow}^+(L_3),$$

$$L_4^+(L_3) = (1/\sqrt{12})[(\phi_1 + \phi_1^*)(\uparrow + \downarrow) + (\phi_2 + \phi_2^*) \\ \times (\omega\uparrow + \omega^*\downarrow) + (\phi_3 + \phi_3^*)(\omega^*\uparrow + \omega\downarrow)],$$

$$L_5^+(L_3) = K L_4^+(L_3),$$

$$L_{6\uparrow}^-(L_2') = (i/\sqrt{6})[(\phi_1 - \phi_1^*) + (\phi_2 - \phi_2^*) + (\phi_3 - \phi_3^*)]\uparrow,$$

$$L_{6\downarrow}^-(L_2') = K L_{6\uparrow}^-(L_2'),$$

$$L_{6\uparrow}^-(L_3') = (i/\sqrt{6})[(\phi_1 - \phi_1^*) + (\phi_2 - \phi_2^*)\omega^* \\ + (\phi_3 - \phi_3^*)\omega]\uparrow,$$

$$L_{6\downarrow}^-(L_3') = K L_{6\uparrow}^-(L_3'),$$

$$L_4^-(L_3') = (i/\sqrt{12})[(\phi_1 - \phi_1^*)(\uparrow - \downarrow) + (\phi_2 - \phi_2^*) \\ \times (\omega\uparrow - \omega^*\downarrow) + (\phi_3 - \phi_3^*)(\omega^*\uparrow - \omega\downarrow)],$$

$$L_5^-(L_3') = K L_4^-(L_3'),$$

where $\omega = \exp\frac{1}{3}(2\pi i)$, \uparrow and \downarrow are spin- $\frac{1}{2}$ wave functions quantized in the $[111]$ direction, and where K is the time-reversal operator which takes the complex conjugate of the spatial part and changes \uparrow to \downarrow and \downarrow to \uparrow .

In the absence of spin-orbit coupling $L_{6\uparrow, \downarrow}^+(L_3)$ states are degenerate with $L_{4,5}^+(L_3)$, and $L_{6\uparrow, \downarrow}^-(L_3')$ states are degenerate with $L_{4,5}^-(L_3')$ so that there are only four bands instead of six. However, because of large spin-orbit coupling in lead salts these degeneracies are lifted with considerable mixing of $L_6^-(L_2')$ and $L_6^-(L_3')$ states which determine the nature of the conduction band and

of $L_6^+(L_1)$ and $L_6^+(L_3)$ states which determine the nature of the valence band. This mixing is responsible for SFR scattering. Apart from $L_{4,5}^-(L_3')$ and $L_{4,5}^+(L_3)$ states, we may write the remaining new eigenstates (see Fig. 1) in the form

$$|CA\alpha\rangle = cL_{6\uparrow}^-(L_2') - dL_{6\downarrow}^-(L_3'), \quad |CA\beta\rangle = K|CA\alpha\rangle, \quad (2.1)$$

$$|CB\alpha\rangle = cL_{6\uparrow}^-(L_3') - dL_{6\downarrow}^-(L_2'), \quad |CB\beta\rangle = K|CB\alpha\rangle, \quad (2.2)$$

$$|VA\alpha\rangle = aL_{6\uparrow}^+(L_1) + bL_{6\downarrow}^+(L_3), \quad |VA\beta\rangle = K|VA\alpha\rangle, \quad (2.3)$$

$$|VB\alpha\rangle = aL_{6\uparrow}^+(L_3) + bL_{6\downarrow}^+(L_1), \quad |VB\beta\rangle = K|VB\alpha\rangle, \quad (2.4)$$

where $a^2 + b^2 = c^2 + d^2 = 1$ and where CA is the bottom of the conduction band and VA is the top of the valence band.

It is convenient at this stage to work in a new coordinate system where the Z axis is parallel to the $[111]$ direction, the X axis is parallel to the $[1\bar{1}2]$ direction, and the Y axis is parallel to the $[1\bar{1}0]$ direction, so that

$$\hat{Z} = (1/\sqrt{3})(\hat{x} + \hat{y} + \hat{z}), \quad (2.5)$$

$$\hat{X} = (1/\sqrt{6})(-\hat{x} - \hat{y} + 2\hat{z}), \quad (2.6)$$

$$\hat{Y} = (1/\sqrt{2})(\hat{x} - \hat{y}). \quad (2.7)$$

In the new coordinate system the nonvanishing matrix elements of $\frac{1}{3}(2m)^{-1/2}\mathbf{e} \cdot \mathbf{p}$, which are approximately equal to the matrix elements of $\frac{1}{3}(2m)^{-1/2}\mathbf{e} \cdot [\mathbf{p} + (\hbar/4mc^2)\boldsymbol{\sigma} \times \nabla V]$, are calculated in the notation⁹ of Lin and Kleinman and given in Table I, with

$$(e_X + ie_Y)/\sqrt{2} = e_+, \quad (e_X - ie_Y)/\sqrt{2} = e_-.$$

III. SPIN-FLIP RAMAN CROSS SECTION

A general expression for the cross section which includes the effect of the Coulomb interaction of the electrons has been derived¹⁰ earlier. In the present case one can, however, treat the electrons to be moving independently in the dc magnetic field and neglect¹¹ the residual Coulomb interaction. In the electric-dipole approximation one then finds the differential scattering cross section per unit solid angle per unit frequency to be given by

$$\frac{d^2\sigma}{d\Theta d\Omega} = r_0^2 \frac{\omega_2}{\omega_1} \int_{-\infty}^{+\infty} \frac{dt}{2\pi} e^{i\Omega t} \langle T_{21}^\dagger(t) T_{21}(0) \rangle \\ = r_0^2 \frac{\omega_2}{\omega_1} \sum_f \sum_i f_0(E_i) [1 - f_0(E_f)] \\ \times \delta(E_f/\hbar - E_i/\hbar - \Omega) |\langle f | t_{21} | i \rangle|^2, \quad (3.1)$$

⁹ Note that matrix elements in Table IV of Ref. 5 are for $i(2m)^{-1/2}\mathbf{k} \cdot \boldsymbol{\pi}$ and not for H' of that paper. Our M_1, M_2 , etc. denote the absolute magnitudes of M_1, M_2 etc. defined in Ref. 5.

¹⁰ S. S. Jha (to be published).

¹¹ P. A. Wolff, Phys. Rev. **171**, 436 (1968).

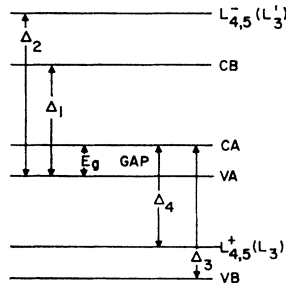


FIG. 1. Energy levels for lead salts at the L point.

TABLE I. Matrix elements of $\frac{1}{3}(2m)^{-1/2}\mathbf{e}\cdot[\mathbf{p}+(\hbar mc^2)\boldsymbol{\sigma}\times\nabla V]$.

	$ CA\alpha\rangle$	$ CA\beta\rangle$	$ CB\alpha\rangle$	$ CB\beta\rangle$	$ L_4^-\rangle$	$ L_5^-\rangle$
$\langle VA\alpha $	(acM_1-bdM_2) $-ie_z$	(adM_3+bcM_5) $-ie_-$	(acM_3-bdM_5) $-ie_-$	(adM_1+bcM_2) $-ie_z$	$(aM_4-bM_8)(1/\sqrt{2})$ $-ie_+$	$(aM_4+bM_8)(1/\sqrt{2})$ $-ie_+$
$\langle VA\beta $	(adM_3+bcM_5) ie_+	(acM_1-bdM_2) $-ie_z$	(adM_1+bcM_2) $+ie_z$	(acM_3-bdM_5) $-ie_+$	$(aM_4+bM_8)(1/\sqrt{2})$ $+ie_-$	(aM_4-bM_8) $-ie_-$
$\langle VB\alpha $	(acM_5-bdM_3) $-ie_+$	(adM_2+bcM_1) $-ie_z$	(acM_2-bdM_1) $-ie_z$	(adM_5+bcM_3) $-ie_+$	$(aM_8-bM_4)(1/\sqrt{2})$ $-ie_-$	$(aM_8+bM_4)(1/\sqrt{2})$ $-ie_-$
$\langle VB\beta $	(adM_2+bcM_1) ie_z	(acM_5-bdM_3) $-ie_-$	(adM_5+bcM_3) ie_-	(acM_2-bdM_1) $-ie_z$	$(aM_8+bM_4)(1/\sqrt{2})$ ie_+	$(aM_8-bM_4)(1/\sqrt{2})$ $-ie_+$
$\langle L_4^+ $	$(cM_6-dM_7)(1/\sqrt{2})$ $-ie_-$	$(cM_6+dM_7)(1/\sqrt{2})$ $-ie_+$	$(cM_7-dM_6)(1/\sqrt{2})$ $-ie_+$	$(cM_7+dM_6)(1/\sqrt{2})$ $-ie_-$	0	M_9 $-ie_z$
$\langle L_5^+ $	$(cM_6+dM_7)(1/\sqrt{2})$ ie_-	$(cM_6-dM_7)(1/\sqrt{2})$ $-ie_+$	$(cM_7-dM_6)(1/\sqrt{2})$ ie_+	$(cM_7+dM_6)(1/\sqrt{2})$ $-ie_-$	M_9 ie_z	0

$$\langle f|t_{21}|i\rangle = \mathbf{e}_2 \cdot \mathbf{e}_1 \delta_{f,i} + m \sum_n \left[\frac{\langle f|\mathbf{v} \cdot \mathbf{e}_2|n\rangle \langle n|\mathbf{v} \cdot \mathbf{e}_1|i\rangle}{(E_i - E_n + \hbar\omega_1)} + \frac{\langle f|\mathbf{v} \cdot \mathbf{e}_1|n\rangle \langle n|\mathbf{v} \cdot \mathbf{e}_2|i\rangle}{E_i - E_n - \hbar\omega_2} \right], \quad (3.2)$$

$$\mathbf{v} = \frac{\mathbf{p}}{m} + \frac{e\mathbf{A}_0}{mc} + \frac{\hbar}{4m^2c^2} \boldsymbol{\sigma} \times \nabla V, \quad (3.3)$$

$$\Omega = \omega_1 - \omega_2, \quad (3.4)$$

$$r_0 = e^2/mc^2,$$

where ω_1 and ω_2 are incident and scattered light frequencies, \mathbf{e}_1 and \mathbf{e}_2 are respective polarizations, \mathbf{A}_0 is the vector potential corresponding to the dc magnetic field, $|i\rangle$, $|n\rangle$, $|f\rangle$ are single-particle electronic wave functions including the spin-orbit effect, and $f_0(E)$ is the Fermi distribution function. For the SFR line $\omega_1 \simeq \omega_2$ at low fields and we may neglect the effect of the field on the scattering amplitude (3.2). Further, the

spin-orbit term in Eq. (3.3) may be ignored and for low concentration of carriers the integrated cross section (per unit volume) at low temperatures may be written as

$$d\sigma/d\Theta = nr_0^2 |\langle f|t_{21}|i\rangle|^2, \quad (3.5)$$

where

$$\langle f|t_{21}|i\rangle \simeq \frac{1}{m} \sum_n \left[\frac{\langle f|\mathbf{p} \cdot \mathbf{e}_2|n\rangle \langle n|\mathbf{p} \cdot \mathbf{e}_1|i\rangle}{E_i - E_n + \hbar\omega_1} + \frac{\langle f|\mathbf{p} \cdot \mathbf{e}_1|n\rangle \langle n|\mathbf{p} \cdot \mathbf{e}_2|i\rangle}{E_i - E_n - \hbar\omega_1} \right]. \quad (3.6)$$

n is the density of electrons available for the particular excitation and where the initial state is assumed to be full and the final state empty. A more general expression valid for higher carrier concentrations and at finite temperatures will be discussed in Sec. V.

In our approximation we may use the matrix elements obtained in Sec. II to obtain the scattering amplitudes for carriers in either the conduction band or the valence band. We find

$$\langle CA\alpha|t_{21}|CA\beta\rangle = -\frac{4i}{3} \left[\frac{(acM_1-bdM_2)(adM_3+bcM_5)(\hbar\omega_1)}{E_g} \left(\frac{E_g^2}{E_g^2 - \hbar^2\omega_1^2} \right) - \frac{(acM_5-bdM_3)(adM_2+bcM_1)(\hbar\omega_1)}{\Delta_3} \left(\frac{\Delta_3^2}{\Delta_3^2 - \hbar^2\omega_1^2} \right) \right] (\mathbf{e}_2 \times \mathbf{e}_1)_-, \quad (3.7)$$

$$\langle VA\beta|t_{21}|VA\alpha\rangle = \frac{4i}{3} \left[\frac{(acM_1-bdM_2)(adM_3+bcM_5)(\hbar\omega_1)}{E_g} \left(\frac{E_g^2}{E_g^2 - \hbar^2\omega_1^2} \right) - \frac{(acM_3-bdM_5)(adM_1+bcM_2)(\hbar\omega_1)}{\Delta_1} \left(\frac{\Delta_1^2}{\Delta_1^2 - \hbar^2\omega_1^2} \right) \right] (\mathbf{e}_2 \times \mathbf{e}_1)_+. \quad (3.8)$$

The values for g_{eff} for these materials are tabulated in Ref. 5. Since both g_{11} and g_1 are positive for the conduction band and negative for the valence band, knowledge of the above amplitudes is sufficient to calculate the scattering cross sections for $g_{\text{eff}}\beta H \gg kT$. The transition amplitudes for reverse processes are related to the above

amplitudes by

$$\langle CA\beta|t_{21}|CA\alpha\rangle = -\langle CA\alpha|t_{21}|CA\beta\rangle^*, \quad (3.9)$$

$$\langle VA\alpha|t_{21}|VA\beta\rangle = -\langle VA\beta|t_{21}|VA\alpha\rangle^*. \quad (3.10)$$

Because of the structure of momentum matrix elements in Table I, it should be noted that in our approximation

TABLE II. Band-edge parameters^a and scattering cross sections.

Semiconductors	M_1 (Ry.) [‡]	M_2 (Ry.) [‡]	M_3 (Ry.) [‡]	M_5 (Ry.) [‡]	E_g (Ry.)	Δ_1 (Ry.)	Δ_3 (Ry.)	a	b	c	d	$ \langle CA\alpha t_{21} CA\beta\rangle $ $\times \langle CA\beta t_{21} CA\alpha\rangle $	$ \langle VA\beta t_{21} VA\alpha\rangle $ $\times \langle VA\alpha t_{21} VA\beta\rangle $	$\frac{1}{n} \frac{d\sigma}{d\Theta}$ (electrons)	$\frac{1}{n} \frac{d\sigma}{d\Theta}$ (holes)
PbTe	0.410	0.306	0.802	0.779	0.014	0.096	0.103	0.974	0.227	0.668	0.744	14.4	14.5	207 r_0^2	210 r_0^2
PbSe	0.464	0.319	0.857	0.788	0.012	0.112	0.146	0.999	0.041	0.864	0.504	24.1	24.0	580 r_0^2	576 r_0^2
PbS	0.467	0.329	0.902	0.848	0.021	0.129	0.149	0.999	0.032	0.881	0.473	5.75	5.6	33.1 r_0^2	31.4 r_0^2

^a Reference 5.

there are no contributions from $L_{4,5}^+$ and $L_{4,5}^-$ intermediate levels to the scattering amplitudes. In the absence of the spin-orbit coupling, $b=d=0$, and scattering amplitudes indeed go to zero. Using the actual values for the mixing coefficients a , b , c , and d , and other band-edge parameters obtained by Lin and Kleinman we have tabulated the numerical values for the magnitude of the scattering amplitudes, apart from the polarization factors, in Table II. The incident frequency is assumed to correspond to 10.6- μ CO₂ laser. For low concentrations the scattering cross sections calculated from Eq. (3.5) are also tabulated. The polarization properties of the scattered wave are obtained from Eqs. (3.7) and (3.8). Note that numerical values for the hole and electron scattering amplitudes are almost the same because they are determined essentially by the first term in Eq. (3.7) and in Eq. (3.8), respectively. For $\hbar\omega_1 \ll \Delta_1, \Delta_3$, only the bottom level of the conduction band (CA) and the top level of the valence band (VA) are important for our calculation. It should also be noted that for further simplification the spin-orbit mixing of the valence band can be ignored since $a^2 \simeq 1$ and $b^2 \simeq 0$.

IV. TWO-BAND APPROXIMATION

In Sec. III we showed that the scattering amplitudes for the incident photon energy $\hbar\omega_1 \ll \Delta_1, \Delta_3$, are sensitive only to two levels near the gap. Numerical values for the amplitudes depend on the spin-orbit mixing coefficients of the conduction and valence bands and on the momentum matrix elements. Since the values of momentum matrix elements in the pseudopotential calculation of Lin and Kleinman⁵ differ quite a bit from the calculation of Conklin, Johnson, and Pratt⁶ based on a true potential, it is worthwhile to investigate the predictions of a strictly two-band model to relate the scattering amplitudes directly to the effective mass and the energy gap.

In a two-band model we consider only the conduction band CA and the valence band VA. Longitudinal (ZZ) and transverse (XX,YY) effective masses of the electrons at the bottom of the conduction band and for the electrons at the top of the valence band are then given by

$$\frac{m}{m_{cl}^*} - 1 = - \left(\frac{m}{m_{vl}^*} - 1 \right) = \frac{4(acM_1 - bdM_2)^2}{3E_g}, \quad (4.1)$$

$$\frac{m}{m_{cl}^*} - 1 = - \left(\frac{m}{m_{vl}^*} - 1 \right) = \frac{2(adM_3 + bcM_5)^2}{3E_g}. \quad (4.2)$$

The predicted ratio of $(m/m_{cl}^* - 1)$ and $(m/m_{vl}^* - 1)$ in our two-band model is fairly well satisfied by experimental results, although actual values are a little different than that obtained from Eqs. (4.1) and (4.2) with the band-edge parameters of Lin and Kleinman.

In a strictly two-band model, ignoring the small contributions from bands other than CA and VA, a comparison of Eqs. (3.7) and (3.8) with Eqs. (4.1) and (4.2) gives

$$\begin{aligned} & \langle CA\alpha|t_{21}|CA\beta\rangle \\ &= \sqrt{2} \left(\frac{m}{m_{cl}^*} - 1 \right)^{1/2} \left(\frac{m}{m_{vl}^*} - 1 \right)^{1/2} \left(\frac{\hbar\omega_1}{E_g} \right) \left(\frac{E_g^2}{E_g^2 - \hbar^2\omega_1^2} \right) \\ & \times \left[\frac{(e_{2X} - ie_{2Y})}{\sqrt{2}} - \frac{(e_{1X} - ie_{1Y})}{\sqrt{2}} e_{2Z} \right], \quad (4.3) \end{aligned}$$

$$\begin{aligned} & \langle VA\beta|t_{21}|VA\alpha\rangle \\ &= \sqrt{2} \left(1 - \frac{m}{m_{vl}^*} \right)^{1/2} \left(1 - \frac{m}{m_{cl}^*} \right)^{1/2} \left(\frac{\hbar\omega_1}{E_g} \right) \left(\frac{E_g^2}{E_g^2 - \hbar^2\omega_1^2} \right) \\ & \times \left[\frac{(e_{2X} + ie_{2Y})}{\sqrt{2}} - \frac{(e_{1X} + ie_{1Y})}{\sqrt{2}} e_{2Z} \right]. \quad (4.4) \end{aligned}$$

The magnitudes of these amplitudes are given in Table III, where we have used the values for $(m/m_{cl}^*) - 1$

TABLE III. Approximate scattering amplitudes based on a strictly two-band model and average^a experimental effective masses.

Semiconductors	m_{cl}^*/m	$-m_{vl}^*/m$	m_{cl}^*/m	$-m_{vl}^*/m$	$ \langle CA\alpha t_{21} CA\beta\rangle $	$ \langle VA\beta t_{21} VA\alpha\rangle $
PbTe	0.24	0.31	0.024	0.022	18.0	18.0
PbSe	0.07	0.068	0.04	0.034	43.5	43.5
PbS	0.105	0.105	0.08	0.075	8.0	8.0

^a See text.

and $(m/m_i^*)-1$ as the average of the experimental values for the respective quantities for the electrons in the conduction and valence bands.

While comparing the predictions of the two-band model with our calculations in Sec. III, it should be kept in mind that while this model is an excellent approximation for the calculation of the SFR scattering amplitudes at low frequencies ($\hbar\omega_1 \ll \Delta_1, \Delta_3$) it is not so good for the effective-mass calculations. Thus the relations (4.3) and (4.4) are crude in the sense that they are expected to give only upper limits for the respective scattering amplitudes.

V. DISCUSSION

From the preceding calculations it is clear that SFR scattering amplitude in lead salts at 10.6μ can be obtained by considering only two bands near the band gap. The numerical values for the cross section are sensitive to the spin-orbit mixing of $L_6^-(L_2')$ and $L_6^-(L_3')$ states which determines the nature of the conduction band and to the mixing of $L_6^+(L_1)$ and $L_6^+(L_3)$ states which determines the nature of the valence band. Since the spin-orbit mixing in the valence band is negligible ($b \approx 0, a \approx 1$) the scattering amplitudes can be written approximately as

$$\begin{aligned} \langle CA\alpha | t_{21} | CA\beta \rangle &\simeq \langle VA\beta | t_{21} | VA\alpha \rangle^* \\ &\simeq -\frac{4i cdM_1 M_3 \hbar\omega_1}{3(E_g^2 - \hbar^2\omega_1^2)} (\mathbf{e}_2 \times \mathbf{e}_1) \end{aligned} \quad (5.1)$$

with $d = (1 - c^2)^{1/2}$. The respective values of the matrix elements M_1 and M_3 are more or less the same in PbTe, PbSe, and PbS. An accurate value for the experimental cross section is not available at present. However, since SFR scattering is a direct measure of the spin-orbit mixing coefficients it should be quite fruitful to measure it in all of these lead salts.

It should be noted that the expression (3.5) is applicable only for low carrier concentrations and at low temperatures. For not very high fields it is still permissible to assume the scattering amplitude to be independent of the magnetic field but in general it is incorrect to assume that only the lowest Landau level $l=0$, with effective spin down for the conduction band and the effective spin up for the valence band, is occupied. In the effective-mass approximation, the one-electron energy in the (111) valley for the magnetic field in the Z direction is given by

$$E_{l, k_Y, k_Z}, S_Z \equiv E_i = E_L + (\hbar^2 k_Z^2 / 2m_i^*) + \hbar(l + \frac{1}{2})(eH/m_i^*c) + g_{11}\beta HS_Z. \quad (5.2)$$

Similar expressions apply to electrons or holes in other valleys¹² with appropriate effective masses and g values.

¹² Since \mathbf{H} is in the Z direction, the effective g value is different for electrons in other equivalent valleys. Thus there are two distinct SFR lines. If θ is the angle of the magnetic field with the

The carrier concentration n in the (111) valley is given by

$$n = \sum_{S_Z} \sum_l \int \frac{dk_Z}{2\pi} \int_{-eH/2c\hbar}^{eH/2c\hbar} \frac{dk_Y}{2\pi} f_0(E_i). \quad (5.3)$$

At $T=0^\circ\text{K}$, approximation (3.5) implies

$$\frac{\hbar^2 k_Z^2(\text{max})}{2(m_i^*)_{\text{eff}}} < \frac{eH}{(m_i^*)_{\text{eff}}c} \hbar, g_{\text{eff}}\beta H,$$

which, for an order of magnitude calculation, may be written approximately as

$$n < (1/\pi^2)(eH/c\hbar)^{3/2}.$$

This requires that for $H=80$ kG, n be less than 10^{17} cm^{-3} and for $H=20$ kG, n be less than 10^{16} cm^{-3} . For higher concentrations upper spin levels of different valleys start getting populated which decreases the cross section. At finite temperatures we must use the expression

$$\begin{aligned} \frac{d\sigma}{d\Theta} &= r_0^2 \sum_l \sum_{S_Z} \left(\frac{eH}{2\pi c\hbar} \right) \int \frac{dk_Z}{2\pi} f_0(E_i) \\ &\quad \times [1 - f_0(E_i + \hbar\Omega)] |\langle f | t_{21} | i \rangle|^2 \end{aligned} \quad (5.4)$$

for the line due to the electrons in the (111) valley, with a similar expression for the line due to the electrons in $(11\bar{1})$, $(\bar{1}11)$ and $(\bar{1}\bar{1}1)$ valleys, where $E_f - E_i = \hbar\Omega$. We can still take the square of scattering amplitude outside the integration sign and use its field-independent value. For a fixed n the variation of $d\sigma/d\Theta$ with H is then given by the integration over joint energy distributions which are oscillatory. A detailed experimental study of the variation of the cross section with H and n and its comparison with the predictions of Eqs. (4.2)–(4.4) should be quite interesting.

In conclusion, it should be noted that we have assumed the momentum transfer $\hbar Q$ from the lightwave to be vanishingly small (long-wavelength limit). Our calculation is valid only if $g_{\text{eff}}\beta H \gg \hbar Q v_f$, where v_f is of the order of the Fermi velocity for the carriers. The problem with no magnetic field ($H \rightarrow 0$) will be discussed in another paper.

ACKNOWLEDGMENTS

The author would like to thank Dr. M. I. Nathan and Dr. P. M. Marcus for helpful discussions.

axis of an ellipsoid, g_{eff} in the valley is given by $g_{\text{eff}}^2 = g_{11}^2 \cos^2\theta + g_{12}^2 \sin^2\theta$. For the $(11\bar{1})$, $(\bar{1}11)$, and (111) valleys $g_{\text{eff}}^2 = \frac{1}{3}g_{11}^2 + (8/9)g_{12}^2$. See, e.g., L. M. Roth, Phys. Rev. **118**, 1534 (1960). By varying the angle θ , one can thus tune the scattered frequency [S. S. Jha and D. V. G. L. N. Rao, Bull. Am. Phys. Soc. **13**, 1640 (1968)].